

# More than two pyrrole tautomers of mesoporphyrin stabilized by a protein

## High resolution optical spectroscopic study

Judit Fidy,<sup>\*</sup> Jane M. Vanderkooi,<sup>†</sup> Juergen Zollfrank,<sup>§</sup> and Josef Friedrich<sup>§</sup>

<sup>\*</sup>Institute of Biophysics, Semmelweis Med. Universitat Budapest, Hungary; <sup>†</sup>Department of Biochemistry and Biophysics University of Pennsylvania, Philadelphia, Pennsylvania 19104, USA; and <sup>§</sup>Institut für Physikalische Chemie, J. Gutenberg Universität, Jakob-Welder Weg 11, Mainz, D-6500 Germany

**ABSTRACT** Mesoporphyrin IX substituted horseradish peroxidase was studied by fluorescence line narrowing and hole burning techniques at cryogenic temperatures. The spectral data reveal that four pyrrole tautomeric configurations of the chromophore are populated within the protein under the influence of irradiation and/or thermal treatment, and the existence of a fifth and a sixth tautomeric configuration is also likely. The relative population of the tautomers changes upon deuterium substitution through modification of the phototransition rate, and also depends on pH, which changes the protonation of neighboring amino acids in the heme pocket. The energy separation of the origins of the tautomers is  $\sim 100 \text{ cm}^{-1}$ . The distribution of barrier heights separating the different tautomeric forms in the ground state and their distribution was determined by temperature cycling hole burning. The distributions can be approximated by Gaussians. The experiment directly yields the distributions on a relative temperature scale, and a model is presented to transform the barrier heights into energy values. It is suggested that the energies for the tautomers are split partially due to the protein crystal field and that the trapping of the tautomeric forms is the consequence of interactions with neighboring amino acids within the heme pocket.

## INTRODUCTION

It is well documented that photochemical holes can be burnt in the absorption spectra of free base porphyrins (for a recent review, see [1]). In the photochemical reaction leading to hole burning, it is generally assumed that during relaxation from the first excited singlet state, the two inner protons rotate simultaneously by  $90^\circ$ , leading to a photoproduct which is stable at low temperatures. This model arose from the observation that in *n*-alkane crystalline hosts, porphin (and also other free base porphyrins of the same symmetry) were found in two different orientations relative to the host, and that these orientations could interconvert under irradiation at cryogenic temperatures (2). Earlier NMR studies showed that in liquids, tautomeric exchange takes place between the intramolecular hydrogen positions, that the stable configurations are those of opposite hydrogen locations, and that ground state exchange between the proton positions ceases at low temperature (3, 4). It was also shown that the two relative orientations for the oppositely located hydrogens in the crystalline matrix lead to two different (0, 0) transition energies (origins) separated by a significant energy difference brought about by a lower symmetry crystal field (2). According to this simple scheme, educt and product in hole burning would form a well defined two state system. The first hole burning experiment based on such a reaction was performed in  $\text{H}_2$ -phthalocyanine (5).

In this work, we substitute free base mesoporphyrin

IX (MP) for the heme in horseradish peroxidase (HRP) and then exploit the photochemical reaction of free base porphyrins to monitor the influence of the polypeptide chain on the porphyrin in the heme pocket. It is important in low temperature spectroscopy to demonstrate that the protein structure is intact. We have shown earlier that MP substitution for the heme in HRP does not destroy its substrate binding ability (6). We also demonstrated that at cryogenic temperatures, the inhomogeneous distribution of (0, 0) energy for MP-HRP is narrow,  $60 \text{ cm}^{-1}$  (7, 8), that is, MP has a well defined location within the protein crevice. The low bimolecular quenching rate of molecular oxygen determined by the fluorescence of protoporphyrin substituted horseradish peroxidase (9) also shows that the heme pocket of this protein has an unusually well protected, rigid structure.

In a recent paper we reported that in broad band (0.1 nm) fluorescence excitation spectra of MP-HRP at 1.5 K several spectral bands can be observed in the (0, 0) region of the  $Q_x$  band. Hole burning experiments in these bands suggested that these bands arise from several origins or species of MP tautomeric forms (8).

In the present paper, it is our goal to investigate the origin of the spectral components of the  $Q_x$  band in more detail by using fluorescence line narrowing (FLN) and temperature cycling hole burning (HB) techniques. We measured the thermal stability of these components, from which we determined the distribution of barrier heights separating the various states. It will be shown that there are more than two tautomeric forms of MP

Address correspondence to Dr. Vanderkooi.

which can be populated at low temperatures photochemically and/or thermally.

Spectral resolution using FLN spectroscopy for monomeric heme proteins was first shown by Angiolillo et al. in 1982 (10); the first HB experiments on proteins were published in 1981 (11, 12). Temperature cycled HB was reported for proteins earlier only in one case, for the phycobilisomes of the algae *mastigocladus laminosus* (13).

## MATERIALS AND METHODS

Horseradish peroxidase C (HRP), a monomeric heme glycoprotein with a molecular weight of  $\sim 34,000$  (14) was used as protein matrix. Of the horseradish peroxidases, isoenzyme C was isolated and purified as described (15). The pure fraction was treated with 2-butanone (16), and the apoprotein was recombined with purified mesoporphyrin IX (MP) (6). The preparation of MP-HRP was performed by Dr. K.-G. Paul (Department of Physiology and Chemistry, University of Umea, Sweden), and kindly donated to our purposes. The stock solution of MP-HRP was stored at 200 K. Samples were prepared in a concentration of 20–40  $\mu\text{M}$  in pH 5, 50 mM ammonium acetate buffers containing 50% glycerol to assure transparency. Deuteration of pyrrole hydrogens was performed by dialysis at 4°C against deuterium oxide at pH 5.

FLN spectroscopy was performed in the temperature range of 5–40 K through the use of a liquid He flow cryostat (APD Cryogenics, Allentown, PA). As tunable laser source, a Coherent 599 linear dye laser pumped by a CW argon ion laser INNOVA 70 (Coherent Inc., Palo Alto, CA) was used. Spectra were measured by a resolution 1  $\text{cm}^{-1}$  through a 1 m Jobin-Yvon double holographic monochromator Ramanor HG2S. For inhomogeneous distribution function determinations a double scanning method (17, 18) was used. This method is based on Eq. 1 which describes the emission intensity of a zero phonon line  $I^{\text{ZPL}}(\nu)$  as:

$$I^{\text{ZPL}}(\nu) = K \epsilon^{\text{ZPL}}(\nu_{\text{exc}}) n(\nu_{0 \leftarrow 0}) f^{\text{ZPL}}(\nu_{\text{em}}) \quad (1)$$

where  $\epsilon^{\text{ZPL}}(\nu_{\text{exc}})$  stands for the absorption probability for a zero phonon excitation in a vibronic state of  $\nu_i = \nu_{\text{exc}} - \nu_{(0,0)}$  vibrational energy,  $f(\nu_{\text{em}})$  is the emission probability for a ZPL transition of  $\nu_{\text{em}}$  energy,  $n[\nu_{(0,0)}]$  is the inhomogeneous distribution function, assumed to be identical for all  $\nu_{(0,0)} + \nu_i$  vibronic levels,  $K$  is a constant. In the experiments,  $\nu_{\text{em}} = \nu_{(0,0)}$ , that is, (0, 0) emission lines were measured. While changing  $\nu_{\text{exc}}$ , only that emission line was followed for which  $\nu_i$  was constant. By this way, not only the emission process, but also the excitation process was kept of the same type, and thus both  $\epsilon$  and  $f$  can be considered constant. Consequently, the only reason why  $I(\nu_{\text{exc}})$  is changing with the excitation energy is that the number of molecules which can be found excited through the chosen vibronic excitation is changing. From this (without superscript ZPL):

$$I(\nu_{\text{exc}}) = K' n[\nu_{(0,0)}]; \quad \text{if } \nu_{\text{exc}} = \nu_i + \nu_{(0,0)}, \quad \text{and } \nu_i = \text{constant}. \quad (2)$$

Thus, the inhomogeneous distribution function  $n$  can be directly measured by the chosen line intensity. This method involves the simplification that the Debye-Waller factor (19), and the vibrational energies in the  $S_1$  state remain constant through the inhomogeneous distribution. Emission spectra in the (0, 0) transition range were measured at different excitation energies varied in steps by 10  $\text{cm}^{-1}$ .  $I(\nu_{\text{exc}})$  data were plotted in dependence of  $\nu_{(0,0)}$ , and Gaussian distribution functions were fitted by computer.

Spectral HB was performed at 1.5 and 4.2 K with a single mode CW-dye laser (Coherent Inc. models INNOVA 90 and 699-21) whose line width was on the order of a few MHz ( $\sim 10^{-3} \text{ cm}^{-1}$ ). The holes for temperature cycling were burnt at 4 K by a power of 10–20  $\mu\text{W}/\text{cm}^2$  to a relative depth of  $\sim 50\%$ ; their line width was  $\sim 0.1 \text{ cm}^{-1}$ . Scanning of the holes was performed by the same laser at lower intensity in the scanning range of 30 GHz ( $\sim 2 \text{ cm}^{-1}$ ). Temperature was adjusted by a liquid He flow cryostat (Leybold-Heraeus VSK 3-300, Koln, Germany). After burning the hole at 4 K, the sample was exposed to temperature cycles in the following way: The temperature of the sample was elevated to a higher value, the so-called excursion temperature, then, after a partial equilibration, it was brought back to 4 K, where the hole shape was measured. Both the linewidth and the hole area may have a characteristic dependence on the excursion temperature ( $T$ ), which is the variable of the experiment. It was shown earlier that the influence of the excursion temperature on the linewidth is decoupled from that on the hole area (20). A previous paper (8) described our line broadening data for MP-HRP in temperature cycling experiments. In the present paper, we focus on the hole area changes (20–22).

The hole area is a measure of the number of molecules in the photoproduct state(s). When the temperature is elevated to the excursion temperature  $T$ , some of the photoproduct molecules are activated, cross the barrier, and return to the educt state. This means that they fill the hole. Hence, the change of the area is proportional to the fraction of photoproduct molecules which have returned to their educt state during a specific cycle. As shown below, the derivative of the hole area with respect to temperature is directly proportional to the probability distribution  $P_V(V)$  of finding a barrier height  $V$ . In brief, the argument is as follows: assume the rate of relaxation  $R$ , from the product to the educt state (separated by a barrier  $V$ ), is governed by an activated process:

$$R = R_0 \exp[-V/kT]. \quad (3)$$

Then, for a certain temperature, there exists a rather well defined marginal barrier  $V_M$  out of the whole distribution, which can just be crossed within the time scale  $\tau$ , the time-roughly-needed to drive the system through the cycle. In the simplest approach (which we call the “ideal glass approximation”) the rate  $R_M$  related to this marginal barrier  $V_M$  is, at the given temperature, determined by the inverse of the experimental time  $\tau$ :

$$R_M \sim \tau^{-1}. \quad (4)$$

The ideal glass approximation is always good in case the dispersion of relaxation rates is large (20). Then from Eqs. 3 and 4,  $V_M$  can be determined:

$$V_M = kT \ln(R_0 \tau). \quad (5)$$

From Eq. 5, we learn that  $V_M$  is almost exclusively determined by the excursion temperature  $T$ . The dependence on the experimental time is only logarithmic. Hence, by varying the temperature, it is possible to probe  $V_M$ . Assume, the experiment is set for a certain temperature  $T$ , which in turn determines a certain  $V_M$ . Those centers having barriers higher than  $V_M$  are, at  $T$ , still in the product state. They make up the hole. Their number  $N_T$  is determined by

$$N_T \sim A_T = \int_{V_M}^{V_{\text{max}}} P_V(V) dV. \quad (6)$$

$A_T$  is the area of the hole at temperature  $T$ , and  $V_{\text{max}}$  is the maximum barrier height. Here  $A_T$  is normalized in a way that  $A_0 = 1$ . Using Eq. 6 together with Eq. 5, it follows that the temperature derivative of  $A_T$  is

proportional to the distribution  $P_V(V)$ :

$$dA_T/dT = k * \ln(R_0\tau) * P_V(V_M). \quad (7)$$

Eq. 7 has been used to determine barrier distributions in glasses, polymers and proteins (20–22). Note that Eq. 7 yields the distributions on a relative scale only.

To determine the barriers on an absolute scale, the factor  $\ln(R_0\tau)$  has to be known. It was shown earlier (20–21), that a value of 30 is an acceptable approximation; this corresponds to a value of  $10^{12} \text{ s}^{-1}$  for  $R_0$ , the attempt frequency. The actual magnitude of  $R_0\tau$  is rather uncritical within a few orders of magnitude due to the log dependence.

There are special advantages in using temperature cycling techniques. First, rather long measuring times may be used to get high signal qualities, because at the low burning/measuring temperature, no further kinetic changes can be expected. Second, returning to the burning temperature sharpens the recovered hole considerably. Consequently, the signal to noise ratio is increased further, and the temperature range available for study can be extended.

## RESULTS

### Production of new spectral bands by irradiation and thermal treatment

Fig. 1 *a* shows the fluorescence excitation spectrum in the  $Q$  band region of MP-HRP at 1.5 K measured by monochromator with a resolution of 3 Å. The spectrum is identical to that at 4 K. The sample was frozen to cryogenic temperatures approximately at a rate of 2 K/s. In the (0,0) range, one origin seems to be largely populated around 6,130 Å; at longer wavelengths, some low intensity peaks can also be observed. At low temper-

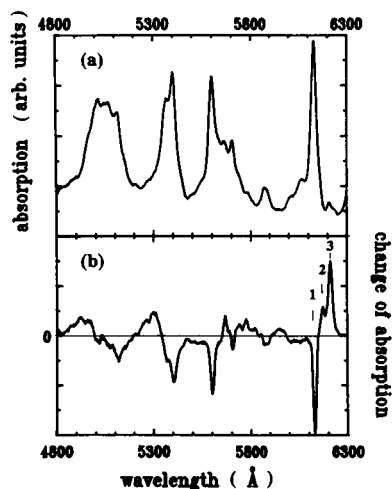


FIGURE 1 (a) Absorption spectrum of MP-HRP at pH 5 and 1.5 K (measured through fluorescence excitation) after sudden freezing from room temperature. Resolution is 3 Å. (b) Change of the absorption spectrum after photobleaching at 6,130 Å (band width 20 Å) for 30 min by an intensity of  $10 \mu\text{W}/\text{cm}^2$ . Tautomer component bands are indicated by numbers.

atures the sample is very sensitive to irradiation. The band at 6,130 Å (peak 1) can almost completely be photobleached. Examples are shown in Fig. 1 *b* and 2; in the latter case, a 50% bleaching was achieved during 30 min by irradiation at 6,130 Å through a monochromator with an intensity of  $\sim 10 \mu\text{W}/\text{cm}^2$  and a bandwidth of 20 Å. The difference spectrum, shown in Fig. 1 *b*, reveals that while the origin of band 1 burns out (we can see the disappearance in the higher vibronics and the  $Q_y$  region, too), two new peaks gain intensity in the (0,0) range marked by 2 and 3. Their vibronics and  $Q_y$  transitions can also be identified by positive signals. It is interesting to note that the  $Q_x$ – $Q_y$  energy separation is bigger for the new products than that of the original component. Thus, irradiation seems to populate new species of MP, leading to characteristic sets of electronic energies.

Fig. 2 shows the (0,0) band region in an expanded scale. In this experiment, the sample freshly frozen from room temperature (spectrum indicated by full line) to 4 K was photobleached leading to the new (0,0) bands 2 and 3 as shown by the dotted line difference spectrum. Subsequently, the sample was heated to higher temperatures, and after a few minutes, returned to 4 K. Then, a spectrum was remeasured. The photobleached feature does not change until  $\sim 30$  K; a spectrum measured after warming up to 25 K totally overlapped with the previous spectrum. However, above 40 K, a new band that gains intensity from the previous products appears (band 4), as shown by the dashed line difference spectrum measured after a temperature rise to 52 K. This spectrum does not change until about somewhat higher than 100 K. By 125 K, all the products have returned to

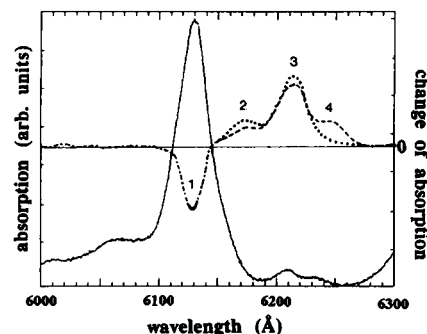


FIGURE 2 Absorption spectrum of MP-HRP at pH 5 measured at 4 K is shown by solid line. Change in the absorption spectrum after photobleaching at 6,130 Å (bandwidth 20 Å) for 30 min by an intensity of  $9.5 \mu\text{W}/\text{cm}^2$ , measured by 4 K (dotted line). The spectrum by dotted line also shows an identical spectrum measured at 4 K after warming the sample up to 25 K. Dashed line indicates two identical spectra taken at 4 K after warming the photobleached sample up to 52 and 72 K. After heating up to 125 K, the spectrum was found identical to the original spectrum at 4 K, shown by solid line.

the original configuration, and we get back the original spectrum shown by solid line at 4 K.

### Identification of the products

In our studies, it was important to make clear that the intensity changes described above represent the phototransformation of different species. For this we had to prove that the bands in question are (0, 0) transitions. This is possible based on the following characteristics. (a) The (0, 0) lines are significantly narrower than those of other transitions. (b) The multiple (0, 0)'s shift with the excitation energy. (c) Their intensity follows the inhomogeneous distribution function of the chromophore population as described in Materials and Methods. In Fig. 3, the (0, 0) range of the FLN spectra is shown for two different excitation energies (Figs. 3 *b*, *c*). No higher energy lines of comparable intensity could be observed. Note that the intensities of multiple (0, 0) lines do not give an estimate for the number of chromophores, because they may originate from simultaneous excitation of different vibronic states. However, it is correct to compare the same kind of spectrum for various conditions (deuteration, pH change). We see that in case of both excitations, the same (0, 0) transitions gain different intensities in these samples indicating that the changed parameters affect the number of molecules characterized by the given emission lines.

It is known from the literature (2, 4) that deuterium substitution for the pyrrole hydrogens significantly slows the phototautomerization process in porphyrins. A factor of 12 was reported for porphyrin in *n*-octane (2). Thus the low intensities around 16,300  $\text{cm}^{-1}$  compared to those around 16,100  $\text{cm}^{-1}$  in undeuterated samples at pH 5, that is, in standard condition (see Fig. 3, *b* and *c*), suggest that during the spectral data collection time of 10 min, significant photochemical changes are induced by the exciting power of 100  $\mu\text{W}$ . The change in the line intensities for standard samples is shown in the inset of Fig. 3 *c* for lines 1 and 2. By comparing the two curves we see different kinetic behavior in the disappearance and the rise of the species. Actually, curve 2 represents the

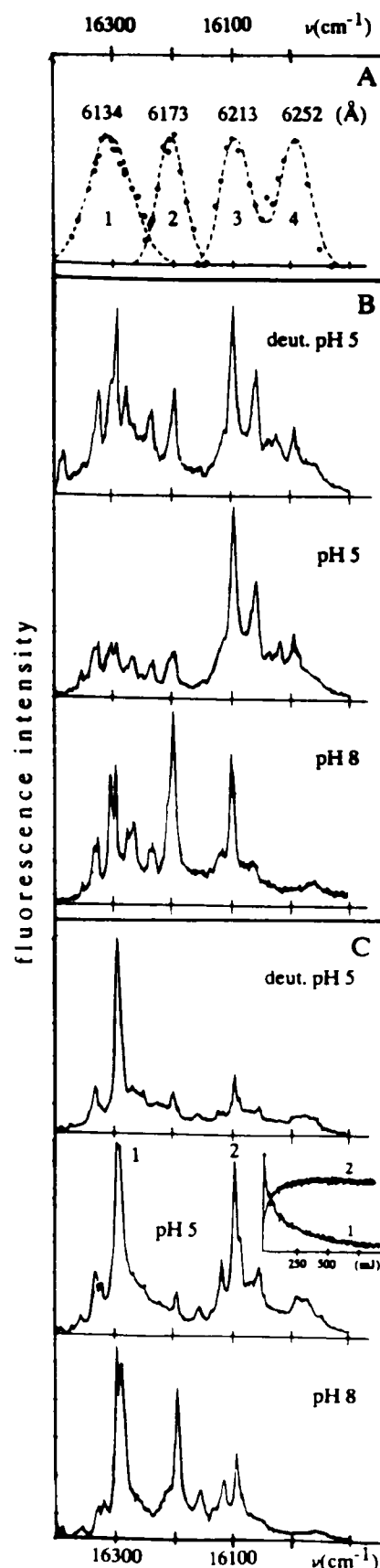


FIGURE 3 (A) Inhomogeneous distribution of (0, 0) transitions for the different tautomeric forms of MP-HRP, indicated by numbers, plotted against the transition energy in  $\text{cm}^{-1}$ . (Corresponding wavelength values for the mean transition energies are shown in A above the distribution functions for comparison with other figures). (B) 0, 0 emission range is shown from the line narrowed spectra of MP-HRP under different conditions when excited at 17,400  $\text{cm}^{-1}$  at 7 K. The exciting power was in the range of 100–500  $\mu\text{W}$ , the data collection time was 8 min. (C) The same range of the spectra is shown as in Fig. 3 B, but now at an excitation energy of 17,500  $\text{cm}^{-1}$ . (Inset) Intensity changes of emission lines at 16,298  $\text{cm}^{-1}$  (curve 1) and at 16,100  $\text{cm}^{-1}$  (curve 2) plotted against the irradiation power in mJ.

formation of a certain group of molecules, and also their further transformation (into bands around 16,000  $\text{cm}^{-1}$ , see 7). Thus, curve 2 is a result of a rising and a slowly decaying process. Comparison of these kinetics with deuterated samples shows slowing by a factor of  $\sim 50$ . Thus the chromophores with (0, 0) energies around 16,300  $\text{cm}^{-1}$  in standard condition are very sensitive to irradiation. They can be almost 100% transformed into other tautomeric forms.

In our earlier FLN studies (7, 18), we did not use excitation powers lower than 30 mW. Thus, in standard MP-HRP samples, the bands around 16,300  $\text{cm}^{-1}$  were immediately photobleached. However, a further phototransformation of the lines around 16,100  $\text{cm}^{-1}$  into a product with (0, 0) energies around 16,000  $\text{cm}^{-1}$  could be seen within a timescale of 20 min. (This product is also represented by low intensities in the spectra shown in this paper.) This lower probability reaction can also be slowed by deuteration but only by a factor of about two.

In samples at pH 8 the population of the states emitting around 16,200  $\text{cm}^{-1}$  is prominent, and the transformation of the species with energies around 16,300  $\text{cm}^{-1}$  is less effective. Also, no further transformation of the lines around 16,100  $\text{cm}^{-1}$  can be induced (7, 23). The influence of deuteration and pH on the tautomerization equilibrium can be exploited to determine the inhomogeneous distributions. In the 16,300  $\text{cm}^{-1}$  range, deuterated samples were used so as not to affect the line intensities by photochemical transformation. For the range around 16,200  $\text{cm}^{-1}$ , pH 8 was used because of the high population of these states. In the lower energy range, samples at standard condition were thoroughly investigated earlier (7, 23). The inhomogeneous distribution functions normalized to the same value are shown in Fig. 3 *a* on the same energy scale as the spectra. Distributions 3 and 4 are taken from our previous studies (7). The origins (mean positions) are shown in *A* above the populations, and also given in Table 1. It is clear that four distinct (0, 0) energy distributions can be detected.

We can summarize the results shown in Figs. 1–3 as follows. Upon irradiation and heat treatment, four different species of MP can be populated in MP-HRP, pH 5 samples. The characteristic (0, 0) energies of the species are separated by  $\sim 100 \text{ cm}^{-1}$ . The width of the corresponding inhomogeneous distributions shown in Table 1 is rather narrow compared to glassy systems, and corresponds with the width of the conventionally measured spectral bands. This latter fact means that phonon wing contributions do not play a significant role in the shape of the spectral bands at low temperatures. This is also seen in the shape of the emission lines of FLN spectra. The photo and thermal interconversion of the species shows that they are structurally related, thus we

TABLE I Parameters of MP tautomeric configurations stabilized by HRP at pH 5: position ( $\mu$ ) and width ( $2\sigma$ ) of inhomogeneous distribution functions for (0,0) transition energy; barrier height distribution position ( $\mu_T$ ) and width ( $2\sigma_T$ ) values determined by fitting with Gaussians

Tautomers	$\mu$	$2\sigma$	$\mu_T$	$2\sigma_T$
	$\text{cm}^{-1}$	$\text{cm}^{-1}$	K (Kcal/mole)	K (Kcal/mole)
1	16,306	80 <sup>a</sup>	> 100 (> 6)	—
2	16,202	50 <sup>b</sup>	—	—
3	16,100	60	9.2 (0.55)	4.2 (0.24)
			19.9 (1.2)	4.4 (0.26)
			> 30	—
4	16,000	60	10.2 (0.61)	1.65 (0.1)
			29.9 (1.8)	8.4 (0.5)

<sup>a</sup>Doublet band; and <sup>b</sup>measured at pH 8 which reduces the width value.

argue that they are different tautomeric forms of MP. This is in line with the deuteration effect, too. At room temperature, almost only one tautomeric form is populated (form 1). Irradiation (through either [0, 0] or vibronic excitation) easily transforms the form 1 MP molecules into 2 and 3. Transformation into form 4 directly from form 1 was not observed. From 2 and 3, form 4 is produced either by heat treatment or by prolonged irradiation. The rate of this transition is much less sensitive to deuteration of the hydrogens than that between 1 and 2–3.

One additional remark should be made. If we look at the spectral features in Fig. 3 around 16,300  $\text{cm}^{-1}$ , under some conditions it can be clearly seen that the lines have a doublet character at both excitation energies (see pH 8 cases; deuteration affects the population of the individual doublets). We performed HB through vibronic excitation as a control for the FLN studies, where vibronic excitation has been applied. The result shown in Fig. 4 proves that an excitation at 5,708 Å in the vibronic range of  $Q_x$  induces hole burning in the (0, 0) band of form 1. Moreover, if we look at the burnt hole in more detail (inset of Fig. 4) we see that the hole bears a doublet feature. The separation of the two holes (7  $\text{cm}^{-1}$ ) coincides with the separation of the doublet (0, 0) lines in the FLN spectra. On this basis we believe that distribution 1 may be an envelope of two populations separated by 7  $\text{cm}^{-1}$ . This interpretation is also supported by the larger width of distribution 1 (Table 1), and the shoulder-like shape of the plot for the distribution in Fig. 3 *a*.

### Hole recovery properties of different tautomeric forms of MP-HRP

Hole recovery processes were studied by temperature cycling experiments in the different tautomeric bands

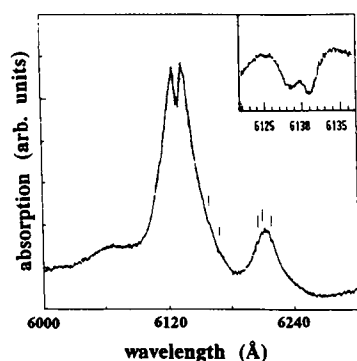


FIGURE 4 Absorption spectrum of MP-HRP irradiated at 5,708 Å by laser light of  $15 \mu\text{W}/\text{cm}^2$  for 10 min. Some of the satellite holes are shown by bars. (Inset) The satellite holes shape at around 6,130 Å is shown on an expanded scale.

using MP-HRP samples at standard conditions. In the experimental series under discussion, the band at 6,173 Å (tautomer 2) was not intense enough to study hole filling for this tautomer. The range in the excursion temperature was limited by hole broadening phenomena (discussed in 8). Reasonable signal/noise conditions could be achieved up to 30 K.

Fig. 5 *a* shows the prominent origin, band 1 at 6,130 Å, at an enlarged scale. The hole is shown as an inset on a further expanded scale. The  $0.03 \text{ Å}$  ( $\sim 0.1 \text{ cm}^{-1}$ ) line-

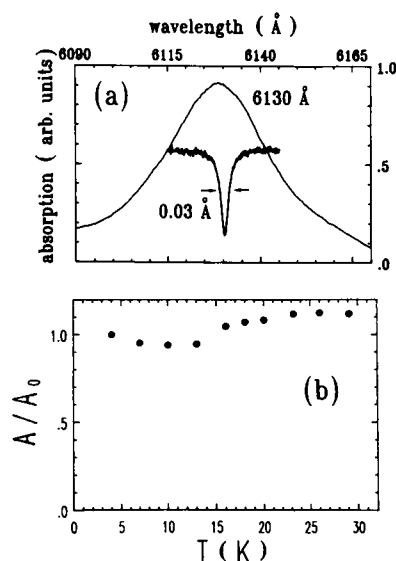


FIGURE 5 (a) Hole burnt in the (0, 0) band for tautomer 1 at 6,130 Å by  $0.15 \mu\text{W}/\text{cm}^2$  burning intensity for 6 min at 4 K, shown on a  $10^3$  times expanded wavelength scale as an inset overlaid on the spectral band. The linewidth of the hole is indicated in Å, the depth was  $\sim 50\%$ . (b) Relative change in the hole area ( $A/A_0$ ) plotted against the excursion temperature ( $T$ ) of a temperature cycling experiment.

width represents the width before any temperature cycling experiments. In Fig. 5 *b*, the hole area is shown on a relative scale as a function of the excursion temperature  $T$ . The data show no significant changes in the hole area up to 30 K, that is, the barriers between product and educt molecules are too high to be crossed in this temperature range. Based on the experiment shown in Fig. 2, however, we may expect that almost all of the holes would recover over 100 K.

Fig. 6 shows the hole filling processes for tautomer 3 (center of site distribution is at 6,213 Å). Because this configuration is scarcely populated at room temperature, it was photochemically enhanced before hole burning by irradiation at 6,130 Å as discussed earlier. The hole within band 3 was burnt at 6,222 Å. Its linewidth before temperature cycling is  $0.034 \text{ Å}$ . Its depth was  $\sim 50\%$ . In Fig. 6 *b* we see that this hole recovers in a complicated fashion; first, around 9 K, a small part of the hole, roughly 20% gets filled, then around 20 K, another filling process gets activated which recovers about 50% of the hole area. The remaining 30% of the hole does not recover within the temperature range of the experiment (30 K). The figure also shows that the data can be fitted sufficiently well by a bimodal Gaussian distribution for the barriers separating the

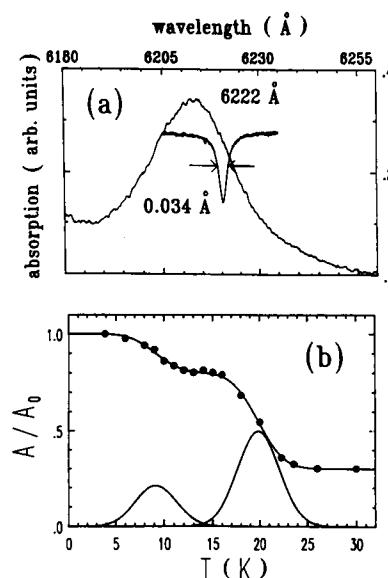


FIGURE 6 (a) Hole burnt in the (0, 0) band for tautomer 3 at 6,222 Å by  $0.5 \mu\text{W}/\text{cm}^2$  intensity for 7 min. at 4 K, shown on a  $10^3$  times expanded wavelength scale as an inset overlaid on the spectral band. The width of the hole is indicated in Å, the depth was  $\sim 50\%$ . (b) Relative change in the area of the hole ( $A/A_0$ ) plotted against the excursion temperature ( $T$ ) of a temperature cycling experiment. The fit curve is an integral over the bimodal Gaussian distribution also shown in the figure. The fitting parameters are given in Table 1.

educt and product states. This distribution is the temperature derivative of the line connecting the data points (see Eq. 8), the fitting parameters are found in Table 1.

Fig. 7 illustrates the behavior of tautomer 4, which we relate to band 4 (center at 6,250 Å). Band 4 was produced by irradiating the sample at 6,130 Å (band 1) and then heating it to 40 K (the spectrum after irradiation is shown in Fig. 7a by a bold line, the other curve shows the production of band 4 by heating). There is strong indication that it grows more at the expense of the 6,173 Å origin than of the origin at 6,134 Å. (The same experiment was discussed in detail earlier in connection with Fig. 2.) Also shown in the figure is the hole burnt into band 4 at 6,250 Å, before temperature cycling. Its depth was around 50%, its linewidth is indicated in the figure. This hole shows also a multistep recovery behavior as seen in Fig. 7b. It recovers by 50% as the temperature is cycled from 4 to 9 K. The rest of the hole seems to recover around 30 K (a barrier distribution centered at 30 K gives satisfactory agreement with the data points). The parameters of the Gaussians are found in Table 1.

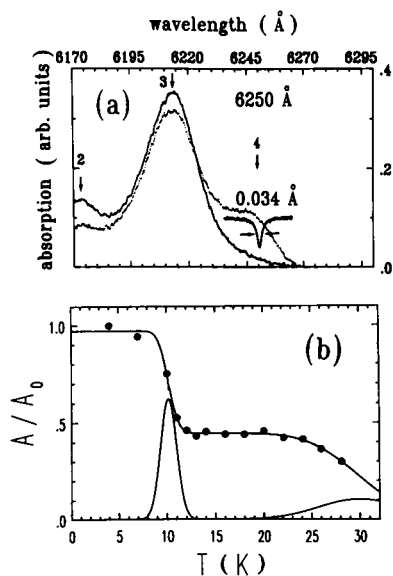


FIGURE 7 (a) Absorption spectrum of a photobleached MP-HRP pH 5 sample at 4 K is shown by solid line. Also shown is the spectrum measured at 4 K after warming the photobleached sample up to 40 K to produce tautomer 4 in the expense of the bands of tautomer 2 and 3. Hole burnt in the (0, 0) band for tautomer 4 is shown on a  $10^3$  times expanded scale as an inset overlaid on the spectral band. The width of the hole is indicated in Å, the depth of the hole was  $\sim 50\%$ . (b) Relative change in the hole area ( $A/A_0$ ) plotted against the excursion temperature of a temperature cycling experiment. The fit curve is the integral over the bimodal Gaussian distribution also shown in the figure. The fitting parameters are given in Table 1.

## DISCUSSION

### Possible tautomeric forms of MP in HRP

It is clear from the data presented in this paper that at low temperature, several tautomeric forms of MP can be populated. The data add to the generally accepted model of two possible linear configurations for the pyrrole hydrogens located at opposite nitrogens. In the literature, including the early NMR studies, it was argued that free base porphyrins may also populate different kinds of configurations with hydrogens at neighboring nitrogens (4). Theoretical works by Sarai (24) revealed characteristic features of the transition between the tautomeric states: at room temperature, synchronous motion of the two hydrogens is of low probability, whereas incoherent hopping is expected. For low temperature, the calculations predict simultaneous hydrogen motions as probable, but do not exclude the successive kind of hydrogen migrations, either. This latter motion was characterized as involving higher energy neighboring positions. In other works, however, these results were debated (25). A theoretical study by Bersuker and Polinger (26) included vibrational mixing of the ground and excited states through vibrations of out of plane symmetry, and came to the conclusion that porphin may have four main stable ground state configurations of equal energy: if one allows for out-of-plane hydrogen positions (one above, and one below the molecular plane), four linear arrangements can be derived. They also support the idea that vibrational mixing by other symmetries may lead to higher energy neighboring positions for the hydrogens. In a recent paper (31), this same model was used to interpret data for porphin in *n*-hexane, and the supposedly neighboring tautomeric forms were characterized by a  $1,800\text{ cm}^{-1}$  higher ground state energy. Versions of out-of-plane hydrogen positions in a linear arrangement (either both above or both below the plane of the porphyrin) instead of the neighboring positions can also be considered. We have detected more conformers than what can be accounted for by the regular inplane versions in a linear arrangement. It is out of the frame of the present study to perform structural identification for these structures. Our present results allow for the conclusion that there are conformers separated by barriers with energies in the range of the forms previously specified as linear. Added to this group, there may be the presence of higher ground state energy structures, and in this second group, perhaps in both, there are structures separated by extremely low barriers in the ground state. Such an

abundance of tautomeric structures was not yet experimentally demonstrated.

We underline that special characteristics of MP in the protein helped to differentiate between its tautomeric forms. These were the following: MP is not of pure  $D_{2h}$  symmetry because of the asymmetric substituents (see Fig. 8), and the effect of this asymmetric substitution is equivalent to having the molecule constantly exposed to an asymmetric crystal field (27). The fact that the chromophore is within a protein means the presence of an additional crystal field of lower symmetry. These effects may lead to a splitting in the electronic energies of the various configurational states, degenerate in an unperturbed geometry (28, 29). The importance of the crystal field of the protein is demonstrated by the observation that MP in alcohol glass (7) or in glycerol (unpublished results) does not show splitting. The high resolution of FLN and HB spectroscopic techniques makes it possible to differentiate the various configurational states, even if their excitation energies differ by as little as a few wavenumbers.

### Barriers separating the tautomeric forms

At moderate and lower temperatures, hydrogen exchange in the ground state is expected to occur by tunneling. The questions, whether it involves synchronous or asynchronous motion, and whether this motion

is coupled to or decoupled from skeletal motions have been debated (24, 25). At different temperatures, different mechanisms were proposed (24). Recent fluorescence studies around 110 K, and a tunneling model interpreting the data lead to ground state energy barrier values of about  $5,000\text{ cm}^{-1}$  between the linear tautomeric forms of porphin in *n*-hexane (31). In interpreting our hole filling data shown in Figs. 5–7, and upon characterizing the ground state barriers between the individual tautomers, we have used the model presented under Materials and Methods. We did not have enough experimental evidence to demonstrate a tunneling processes in the studied temperature range. The non-Arrhenius behavior of the tautomeric conversion kinetics reported elsewhere (7) can be well interpreted as a result of barrier distribution.

From temperature cycling HB studies on phthalocyanine in *n*-octane (30), and from what was estimated on the basis of NMR, IR and fluorescence studies (4, 24, 25, 31) for symmetric porphyrins, we estimate an average barrier height between regular linear tautomers on the order of  $4,000\text{ cm}^{-1}$  (11.4 kcal/Mol). (This value was involved in our model to interpret the hole filling data.) We found a population (or two): form 1, separated from the others by high barriers of about this magnitude dominating at room temperature, thus we concluded that this linear form has the lowest ground state energy.

Most of the holes burnt into tautomer 3 are filled from a state separated by a barrier on the order of 20 K. This result, compared to previous temperature cycling studies on tautomers 3 and 4 (22), suggest that the 20 K barrier separates tautomers 3 and 4. The remaining hole area, not refilled below 30 K, most probably arise from those tautomers which were transformed into form 1, in correspondence with the results shown in Fig. 2.

The hole burnt into the population corresponding to tautomer 3 was, at  $6,222\text{ Å}$ , a little bit toward the population for tautomer 4 (see the inhomogeneous distribution functions in Fig. 3 *a*), thus it may be that some molecules of type 4 are simultaneously transformed during burning. This queries unambiguous connection of barriers around 9 K (Fig. 5 *b*) with tautomer 3. A similar barrier height population is also found in tautomer 4 to a large extent. However, the possibility can not be excluded that the tautomeric state 3 has another neighboring state separated by a barrier on the order of 9 K, in addition to the configurations 1 and 4.

The hole burnt into the tautomer 4 population reveals that about half of this configuration is transformed into a form separated by a low barrier ( $\sim 9\text{ K}$ ), similar to that observed by a small percent in the hole filling for tautomer 3. As for the fitted width of the Gaussian, we believe that we may rely more on the width value

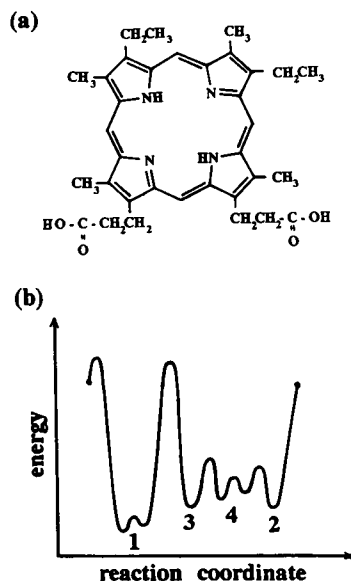


FIGURE 8 (a) Structure of mesoporphyrin IX. (b) Ground state energy landscape of MP-HRP at pH 5. Energy valleys corresponding to the tautomeric forms are indicated by numbers.



determined in the case of tautomer 3 in the same range as  $\sim 4$  K. The area filling that becomes observable above around 22 K may be a process used to populate form 4 by heat treatment (at 40 K) from forms 2 and 3. The large width of this distribution also suggest that this hole filling is a composite phenomenon.

### Comments on the Gaussian distribution of barrier heights

The hole recovery data demonstrate that the distribution of barrier heights for the various tautomeric conformers of MP in a protein crevice is sufficiently well described by Gaussians. A Gaussian distribution, suggested by Stein (33) was, for example, found by Berendzen and Braunstein (34) for the geminate recombination of deligated carbonmonoxymyoglobin. (A discussion of the effect of inhomogeneous distribution of molecules on the reaction kinetics of the myoglobin system is given by Austin and coworkers [35]). In another system, the recovery reaction of photochemical holes burnt into a phthalocyanine doped Shpol'skii crystal is well modeled by a Gaussian distribution of barrier heights (30). However, for quite a large series of doped glasses and polymers (34), a highly asymmetric distribution was found, following closely a so called Porter-Thomas distribution (36).

Recently, Laird and Skinner published a microscopic theory on inhomogeneous line broadening (37) of dye probes in glasses. They were able to show under what conditions Gaussian distributions prevail. Because the distribution of barrier heights is the consequence of the same phenomenon as inhomogeneous line broadening, one can use their theory to investigate the conditions under which Gaussian distribution is expected for barrier heights. Basically, three requirements have to be met: (a) A zero order barrier of the reacting species has to be present onto which the solvent can act as a perturbing environment. (b) All possible configurations of the solvent molecules should be statistically independent. This means that the  $N$ -particle density correlation function can be factorized into a product of  $N$  two-particle correlation functions. Then, the huge number of possible configurations can interact independently with the zero order barrier leading to a random modulation. To get a distribution of barriers it is important that the interaction of the solvent configurations with the minimum energy state along the reactive hypersurface is not completely correlated with the corresponding maximum energy state. (c) The third condition necessary for a Gaussian distribution is a sufficiently high density of the solvent.

It seems to be clear that some of these restrictions are quite severe, for instance, the assumption that there is

no correlation between configurations of the solvent molecules. It could be due to this restrictive condition that some of the measured distributions are not quite Gaussians but show pronounced asymmetries. In contrast, most of the doped glass systems, where the distribution of reactive barriers followed a sort of Porter-Thomas type distribution, are characterized by photophysical hole burning processes. Photophysical hole burning takes place when the dye probe itself is not photoreactive. In this case, there is no zero-order barrier. Instead, the barrier has to be built up by the solvent molecules. It is then clear that one of the above requirements is not met, namely, that the solvent molecules are totally uncorrelated. Several solvent molecules have to act together to establish some configurational barrier for the dopand molecule. It seems that a situation like this occurs in some of the photosynthetic antenna pigments (22). In this case, the recovery curve of a spectral hole could be modelled as being a superposition of a Gaussian and a Porter-Thomas distribution, possibly due to a simultaneous photophysical and photochemical burning process. In the case of MP-HRP, the photoreaction is based on pyrrole hydrogen transformation, and hence, there is a zero order reaction barrier for the isolated probe species. Provided that there is a sufficiently large region in phase space where the protein configurations can be considered as being independent, a Gaussian distribution function can be expected.

### Characterization of MP tautomers stabilized by HRP at pH 5 at cryogenic temperatures

The conventional and FLN studies at cryogenic temperatures reported in this paper for MP in HRP reveal that at pH 5 at room temperature the porphyrin is present in two, about equally populated pyrrole tautomeric configurations showing only little (in the order of  $10\text{ cm}^{-1}$ ) energy separation (see results of doublet lines) in their  $S_1^0 \rightarrow S_0^0$  transition energies. These (0, 0) energies are around  $6,134\text{ Å}$  (form 1 *a* and 1 *b*). Irradiation into this configuration at low temperature leads with high probability to the formation of a stable conformer with (0, 0) band maximum at  $6,213\text{ Å}$  (form 3), and with less probability to a configuration with (0, 0) band maximum around  $6,173\text{ Å}$  (form 2). At pH 8, this latter form is also significantly populated at room temperature along with those with  $6,134\text{ Å}$  transition energy. The photochemical transformation from forms 1 to 3 and 2 at pH 5 is very sensitive to deuterium substitution, and the barrier heights in ground state isolating forms 1 from the others correspond to those expected between linear tautomeric

forms. Thus, we believe that forms 1 *a* and 1 *b*, and forms 2–3 represent different linear configurations.

We argue that the tautomer 4 ([0, 0] bands at 6,252 Å) represent a peculiar group of tautomers. They can be produced from form 1 through forms 2 and 3 with about three orders of magnitude less probability by irradiation at low temperature. The phototransformation rate from 2 and 3 to form 4 is only moderately sensitive to deuterium substitution for the pyrrole hydrogens. Form 4 can also be populated from forms 2 and 3 by heating the sample up to 40 K. By warming to above 100 K, the MPs will be brought back to the original room temperature configuration, forms 1 *a* and 1 *b*. We suggest that type 4 molecules are similar to those that others (31) have found that have higher ground state energies in case of porphin in *n*-hexane. The low barrier heights found around 9 K may separate two such configurations of similar symmetries.

The results summarized above lead to the landscape schematized in Fig. 8 *b* for the ground state of MP in pH 5 HRP. The model shown in the figure is a circular (multidimensional) energy valley arrangement simplified to be linear by “cutting” it along the reaction coordinate scale. A similar model was presented by Bersuker and Polinger (26), with identical energy valleys for a symmetric porphyrin without crystal field effects. It is the consequence of the asymmetric environment imposed by the protein as well as the asymmetry of the porphyrin that makes our model more complicated. The results showed also that pH changes may change the protonation of the surrounding amino acids (histidines), and this leads to restrictions in the stabilized MP tautomeric forms. Thus, for high pH, another energy “landscape” might hold. Form 4 positions would be excluded, and the ground and excited state energy landscape is affected in a way that form 2 gets significantly populated.

Finally, we would like to underline that this paper is a report about the existence of new forms of a free base porphyrin within a protein. The results do not give direct information about the nature of the protein matrix (such results are discussed in 8). However, indirectly, characteristics of the heme pockets are involved in the observed phenomena at the following points. (*a*) The Q band energies for the tautomers are split partially due to the protein crystal field; (*b*) The energy landscape shown in Fig. 8, and thus the trapping in the tautomeric forms is the consequence of the neighboring amino acid groups within the pocket; (*c*) The unusually narrow inhomogeneous distribution of the (0, 0) bands which helped to differentiate the conformers is due to the special character of the heme pocket in HRP.

The authors thank the Deutsche Forschungsgemeinschaft (grants Fr456/12-1 and SFB262-D12), the United States National Science Foundation (grant DM 88-15723) and the Semmelweis University of Medicine, Budapest for financial support.

Received for publication 13 February 1991 and in final form 2 October 1991.

## REFERENCES

- Voelker, S. 1989. Spectral hole-burning in crystalline and amorphous organic solids. Optical relaxation processes at low temperature. In *Relaxation Processes in Molecular Excited States*. J. Fuenfschilling, editor. Kluwer Academic Publishers, The Netherlands. 113–242.
- Voelker, S., and J. H. van der Waals. 1976. Laser induced photochemical isomerization of free-base porphyrin in an *n*-octane crystal at 4.2 K. *Mol. Phys.* 32:1703–1718.
- Storm, C. B., and Y. Teklu. 1972. Nitrogen-hydrogen tautomerism in porphyrins and chlorins. *J. Am. Chem. Soc.* 94:1745–1747.
- Abraham, R. J., G. E. Hawkes, and K. M. Smith. 1974. N-H tautomerism in porphyrins: an NMR study. *Tetrahedron Lett.* 16:1483–1486.
- Gorokhovskii, A. A., R. K. Kaarli, and L. A. Rebane. 1974. Spectral hole burning in a Spolskii system (Russ). *J. Exp. Theor. Phys. Lett.* 20:474–479.
- Horie, T., J. M. Vanderkooi, and K.-G. Paul. 1985. Study of the active site of horseradish peroxidase isoenzymes A and C by luminescence. *Biochemistry*. 24:7931–7935.
- Fidy, J., K.-G. Paul, and J. M. Vanderkooi. 1989. The mechanism of photoautomerisation in mesoporphyrin horseradish peroxidase. Studies by fluorescence line narrowing spectroscopy. *J. Phys. Chem.* 93:2253–2261.
- Zollfrank, J., J. Friedrich, J. M. Vanderkooi, and J. Fidy. 1991. Conformational relaxation of a low temperature protein as probed by photochemical hole burning: horseradish peroxidase. *Biophys. J.* 59:305–312.
- Brunet, J. E., C. Julian, and D. M. Jameson. 1990. Oxygen diffusion through horseradish peroxidase. *Photochem. Photobiol.* 51:487–489.
- Angiolillo, P. J., J. S. Leigh, and J. M. Vanderkooi. 1982. Resolved fluorescence emission spectra of iron-free cytochrome *c*. *Photochem. Photobiol.* 36:133–137.
- Friedrich, J., H. Scheer, B. Zickendracht-Wendelstadt, and D. Haarer. 1981. Photochemical hole burning: a means to observe high resolution optical structures in phycoerythrin. *J. Chem. Phys.* 74:2260–2266.
- Friedrich, J., H. Scheer, B. Zickendracht-Wendelstadt, and D. Haarer. 1981. High resolution optical studies on C-phycoerythrin via photochemical hole burning. *J. Am. Chem. Soc.* 103:1030–1035.
- Koehler, W., and J. Friedrich. 1989. Probing of conformational relaxation processes of protein by frequency labeling of optical states. *J. Chem. Phys.* 90:1270–1273.
- Dunford, H. B. 1982. Peroxidases. *Adv. Inorg. Chem.* 4:41–68.
- Paul, K.-G., and T. Stigbrand. 1970. Four isoperoxidases from horseradish root. *Acta Chem. Scand.* 24:3607–3617.
- Teale, F. W. J. 1959. Cleavage of the hemoprotein link by acid methyl ethyl ketone. *Biochim. Biophys. Acta.* 35:543–000.

17. Fuenfschilling, J., I. Zschokke-Granacher, and D. F. Williams. 1981. The determination of the site energy distribution of organic molecules dissolved in glassy matrices. *J. Chem. Phys.* 75:3669–3673.
18. Fidy, J., K.-G. Paul, and J. M. Vanderkooi. 1989. Differences in the binding of aromatic substrates to horseradish peroxidase revealed by fluorescence line narrowing. *Biochemistry.* 28:7531–7541.
19. Personov, R. I. 1983. Site selection spectroscopy of complex molecules in solutions and its applications. In *Spectroscopy and Excitation Dynamics of Condensed Molecular Systems*. V. M. Agranovich and R. M. Hochstrasser, editors. North Holland, Amsterdam. 555–619.
20. Koehler, W., J. Zollfrank, and J. Friedrich. 1989. Thermal irreversibility in optically labelled low temperature glasses. *Phys. Rev.* B39:5414–5423.
21. Koehler, W., and J. Friedrich. 1987. Distribution of barrier heights in amorphous organic materials. *Phys. Rev. Lett.* 59:2199–2202.
22. Koehler, W., J. Friedrich, and H. Scheer. 1988. Conformational barriers in low temperature proteins. *Phys. Rev.* A37:660–662.
23. Fidy, J., H. Koloczek, K.-G. Paul, and J. M. Vanderkooi. 1987. The pH dependence of phototautomerism in horseradish peroxidase monitored by fluorescence site selection spectroscopy. *Chem. Phys. Lett.* 142:562–566.
24. Sarai, A. 1982. Dynamics of proton migration in free base porphyrins. *J. Chem. Phys.* 76:5554–5563.
25. Limbach, H.-H., J. Henning, and J. Stulz. 1983. IR spectroscopic study of isotope effects on the NH/ND—stretching bands of meso-tetraphenylporphyrin and vibrational hydrogen tunneling. *J. Chem. Phys.* 78:5432–5436.
26. Bersuker, G. I., and V. Z. Polinger. 1984. The pseudo Jahn-Teller dynamics of central protons in porphyrins. *Chem. Phys.* 86:57–65.
27. Hoffman, B. M., and M. A. Ratner. 1987. Jahn-Teller effects in metalloporphyrins and other four-fold symmetric systems. *Mol. Phys.* 35:901–925.
28. Jahn, H. A., and E. Teller. 1936. Stability of degenerate electronic states in polyatomic molecules. *Phys. Rev.* 49:874–900.
29. Bersuker, I. B., and S. S. Stavrov. 1988. Structure and properties of metalloporphyrins and hemoproteins: the vibronic approach. *Coord. Chem. Rev.* 88:1–68.
30. Zollfrank, J., and J. Friedrich. 1990. Spectral diffusion and thermal recovery of spectral holes burnt into a phthalocyanine doped Shpol'skii system. *J. Chem. Phys.* 93:8586–8590.
31. Butenhoff, T. J., and C. B. Moore. 1988. Hydrogen atom tunneling in the thermal tautomerism of porphin imbedded in an n-hexane matrix. *J. Am. Chem. Soc.* 110:8336–8341.
32. Stein, D. L. 1985. A model of protein conformational substates. 1985. *Proc. Natl. Acad. Sci. USA.* 82:3670–3672.
33. Berendzen, J., and D. Braunstein. 1990. Temperature derivative spectroscopy: a tool for protein dynamics. *Proc. Natl. Acad. Sci. USA.* 87:1–5.
34. Austin, R. H., K. W. Beeson, L. Eisenstein, H. Frauenfelder, and I. C. Gunsalus. 1975. *Biochemistry.* 145:5355–5373.
35. Porter, C. E., and R. G. Thomas. 1956. Fluctuations of nuclear reaction width. *Phys. Rev.* 104:483–491.
36. Laird, B. B., and J. L. Skinner. 1989. Microscopic theory of reversible pressure broadening in hole burning spectra of impurities in glasses. *J. Chem. Phys.* 90:3274–3281.